TASK QUARTERLY 9 No 1, 81–102

SIMULATIONS OF FLOW PATTERNS IN SILOS WITH A CELLULAR AUTOMATON: PART 1

JAN KOZICKI AND JACEK TEJCHMAN

Civil Engineering Department,
Gdansk University of Technology,
Narutowicza 11/12, 80-952 Gdansk, Poland
tejchmk@pg.gda.pl

(Received 12 May 2004; revised manuscript received 16 August 2004)

Abstract: A simplified cellular automaton was used to calculate the kinematics of non-cohesive granular materials during confined flow in silos. In this model, granular flow was assumed to be an upward propagation of holes through a lattice composed of cells representing single particles. Calculations were carried out with different silo shapes and inserts, transition probabilities, migration rules, outflow schemes, grid types, wall roughness and cell numbers. To visualize the calculation process, horizontal layers of various shades were introduced. The simulation results were compared with laboratory tests in model silos.

Keywords: cellular automaton, granular flow, flow pattern, insert, silo

1. Introduction

The cellular automata approach is a powerful method to describe, understand and simulate the behavior of complex physical systems, which are difficult to describe using the more traditional approaches (by means of differential equations). It is viewed as an alternative form of the microscopic reality, which exhibits the expected macroscopic behavior [1]. The concept dates back to the 1950's [2, 3]. During the next fifty years of applications, cellular automata have been developed and used in many fields of physics, chemistry and biology dealing with the fluid flow [1, 4]. They have also been used to simulate the behavior of granular materials during vibration, piling, toppling, segregation, displacement of retaining walls and rapid flow [1, 5–21]. In models, collisions, friction, rotations and particle size have been introduced. Cellular automata have been used to simulate rapid flow in silos [5, 13–21] as above the outlet silo fills behave more like fluids rather than solids (although the internal friction of the bulk material is still of major importance [22]).

Cellular automata have both advantages and disadvantages relative to other modeling techniques. The advantages include large numbers of particles, lack of restrictions for deformations, simplicity of implementation and small amounts of computer time needed to describe the flow. The behavior is described not in terms of differential equations but in discrete systems. The models provide insight into the main

physical features of flow on microscopic and macroscopic level. The main disadvantage is that the models are purely kinematic and no flow dynamics is involved.

The objective of simulations presented in this paper was to determine flow patterns of non-cohesive granular bodies in model silos, with or without inserts, using a simplified cellular automaton. A realistic prognosis of flow patterns of bulk solids is very important when designing silos [23–27] since loads in silos are directly related to the flow type. The flow of bulk material stored in silos is of two main patterns: funnel flow (core flow) and mass flow. In mass flow, the entire material is in motion during discharge. In funnel flow, movement occurs only in a channel within the stored material surrounded by non-flowing material. Cellular automata simulations have been carried out with different silo shapes, migration rules, transport schemes, transition probabilities, outflow velocities, wall roughness and cell numbers. Most often a two-dimensional array of square cells was used. However, comparative calculations have also been carried out with a three-dimensional grid of square cells. Four different types of inserts (often used in the silo industry) have mainly been taken into account: a wedge-shaped cone, an internal hopper, two inclined discharging tubes over the outlet, and a perforated vertical emptying tube.

2. Description of the model

A cellular automaton requires a lattice of adjacent cells covering a portion of a d-dimensional space, a set of variables attached to each site of the lattice and giving the local state of each cell at time $t = 0, 1, 2, \ldots$, and a rule which specifies the variables' evolution in time [1]. Thus, a cellular automaton is a system composed of adjacent cells (usually organized as a regular hexagonal, triangular or rectangular lattice), which evolves in a discrete time step. Each cell is characterized by an internal state whose value belongs to a finite set. These states are updated in parallel according to local rules involving the neighborhood of each cell. In the simplified cellular automaton discussed in this paper, granular flow of separate grains in silos is described as upward propagation and diffusion of holes through the lattice of cells (grains move downwards and voids move upwards). Each cell may be empty or filled by a particle of the material. The computation process involves searching through all lattice cells for holes. At each time step, a particle flowing downwards due to gravity can move from one cell to an empty neighboring cell or remain at rest. The filling of one cell causes the formation of a new empty one, which is again filled with a randomly chosen particle. Thus the migration of holes inside the granular materials occurs. The transition of holes corresponds to the transport of the material in the opposite direction. The evolution rule describing the state change can be deterministic or probabilistic. For silo flow, it is usually assumed to be probabilistic, similarly as in a real bulk solid where the shapes and dimensions of particles, contact points and forces between particles, and particle roughness are completely random. The phenomena of collision, friction and rotation have not been taken into account in the model.

Baxter *et al.* [13, 14] have simulated a two-dimensional deterministic process of filling and flow of granular material in a hopper using a regular triangular array of cells. The direction of grain displacement corresponded to the direction in which mechanical energy was minimal. The energy consisted of two components: gravity

and interaction between neighboring grains, including friction, dilatancy and relative orientation of stick-like grains.

Peng and Herrmann [6] investigated density waves during granular flow in a pipe with an improved cellular automaton. In their model, inelastic collisions of particles were taken into account (conserving mass and momentum), similarly as in a lattice-gas automaton [4]. Particles could change their velocities during collisions and move during propagation in the direction of their velocities to neighboring sites, where they collided again. The four material parameters assumed were related to gravity, dissipation, density and wall roughness.

The model used for silo flow in [18–20] was based on the transmission of the weight of grains by different migration rules (so-called frontal, interstitial and constrictive).

Savage [15, 16] used a simple probabilistic cellular automaton with regular rectangular cells to describe two-dimensional flow in a hopper. An empty cell could be filled by particles from 3 cells located in the horizontal layer above. The aspect ratio of cells was changed to model the internal friction angle of the silo fill. However, too large diffusion of particles was observed in the calculations. In a similar two-dimensional cellular model by Osinov [17] with a square grid of cells, an empty cell could be filled by particles from 3 cells (one above, the others at the sides). The transition probabilities and dimensions of cells were the governing parameters affecting the hopper flow process. In addition, the simulations took into account loosening of the material (flowing particles could generate their copies).

In all the above mentioned simulations of silo flow [13–21], agreement with laboratory tests was surprisingly good in spite of the extreme simplicity of cellular automata models neglecting the dynamics of the granular flow process.

3. Simulation results

As compared with the calculations of silo flow with a similar simplified cellular automaton [15–17], other migration rules and transition probabilities were tested and different types of cell grids were compared. The calculations were also carried out with transition probabilities dependent on cell location to simulate walls of varied roughness. Moreover, various outflow velocities were simulated.

The simulations were carried out with various:

- silo shapes,
- particle numbers,
- migration rules,
- transition probabilities,
- transport schemes,
- outlet velocities,
- wall roughness,
- lattice grids, and
- silo inserts.

Four different migration rules were investigated using a quadratic grid of cells (Figure 1). In the first and second case (rule **A** and **B**), each empty quadratic cell could be filled by particles from 3 or 5 cells located in the horizontal layer above. In the

third case (rule **C**), each empty cell could be filled by particles from 3 cells located above and at the sides. In the fourth case (rule **D**), each empty cell was filled by particles from 5 cells located above and at the sides. The probability of hole transport from one cell to another was assumed to be p_i ($\sum p_i = 1$) and did not depend on coordinates.

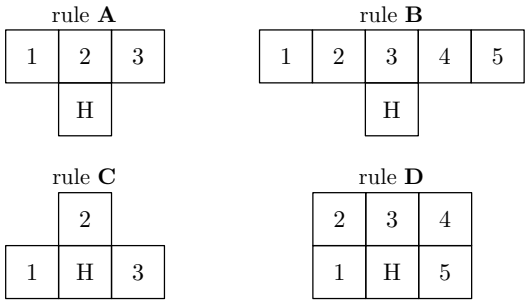

Figure 1. Migration rules assumed for a two-dimensional array of quadratic cells (H – void)

To take into account the effect of the transport scheme, the so-called 'disturbed' flow was taken into account. In this case, the motion of empty cells (without particles) was also considered during flow. They propagated similarly to filled cells (containing particles). To capture material loosening (dilatancy), each particle passing through a certain number of cells (*e.g.* 100) was assumed to generate its copy in a hole to be filled [17]. Thus, the material's volume could grow during flow.

To simulate outflow with a constant outlet velocity, the filled cells were not emptied every calculation step but *e.g.* every 5 steps.

To model very rough walls, different transition probabilities were assumed in the wall region compared to the remaining region.

The calculations were performed with a square and hexagonal grid of cells. Hexagonal cells are usually used to simulate a Navier-Stokes equation of fluid flow [1]. They are preferable because of isotropy of the momentum advection tensor.

3.1. Effect of migration rules and transition probabilities

To find the most realistic migration rule for granular flow in silos, simulation results were compared with results of simple laboratory model tests carried out with a mass flow silo and a funnel flow silo (without inserts) made of perspex. The dimensions of the mass flow silo were: 0.32m (height) by 0.09m (width) by 0.07m (length). The wall inclination of the hopper against the bottom was 60°. The dimensions of the funnel flow silo were: 0.28m (height) by 0.15m (width) by 0.07m (length). The wall inclination of the hopper was 30°. The silos contained dry sand with a mean grain diameter of 0.5mm. The outflow was due to gravitation. The experimental flow patterns during mass and funnel flow are shown in Figure 2.

The effects of the migration rules and transition probabilities are shown in Figures 3–10 for the mass flow silo and the funnel flow silo using 50 000 cells (Figure 2b). The dimensions of the cells were $1 \times 1\,\mathrm{mm}^2$. In addition, diagrams are attached indicating the amount of particles moving through each cell (darker regions denote greater numbers of flowing particles). The distribution of the transition

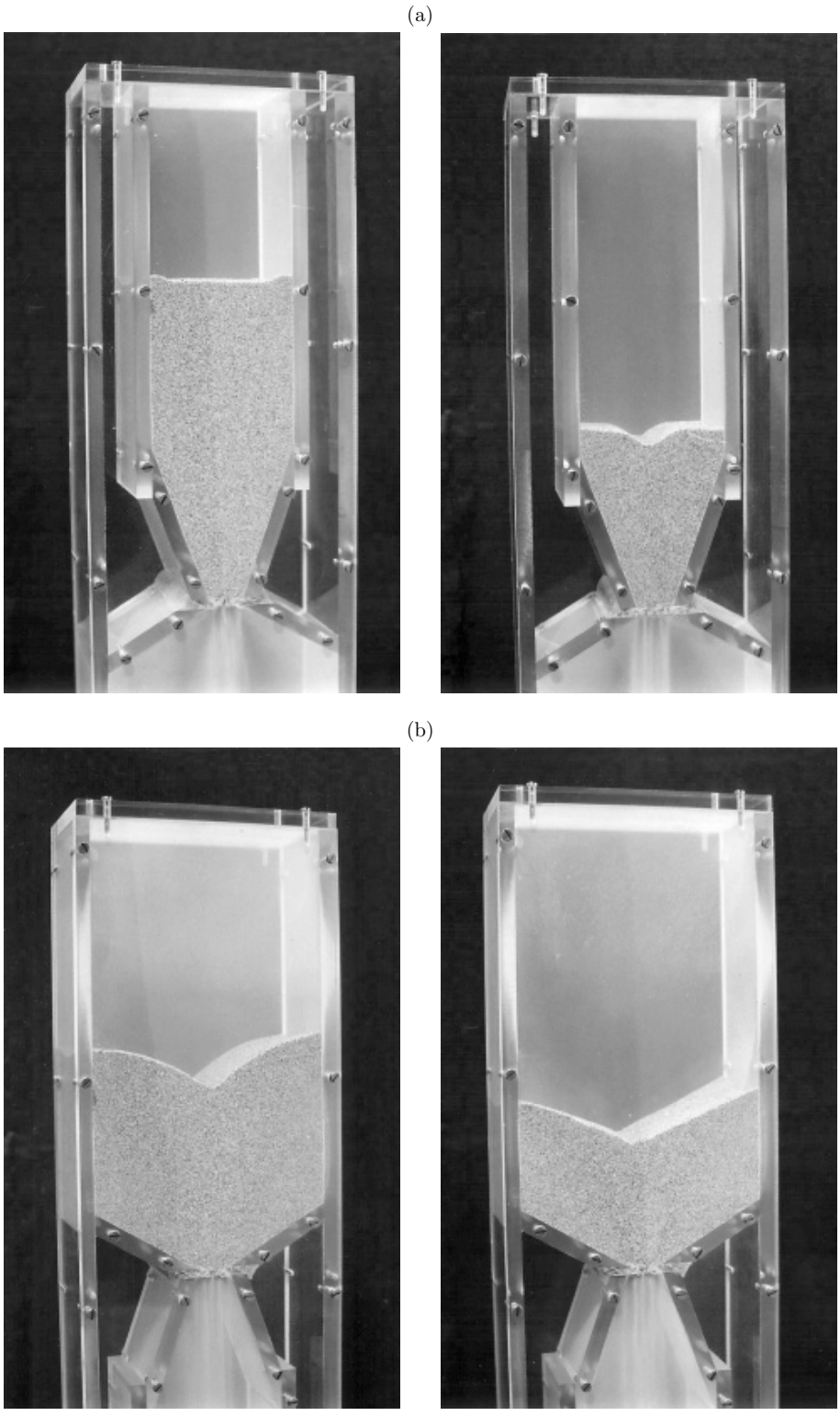

Figure 2. Flow patterns observed in model silo tests: (a) mass flow; (b) funnel flow

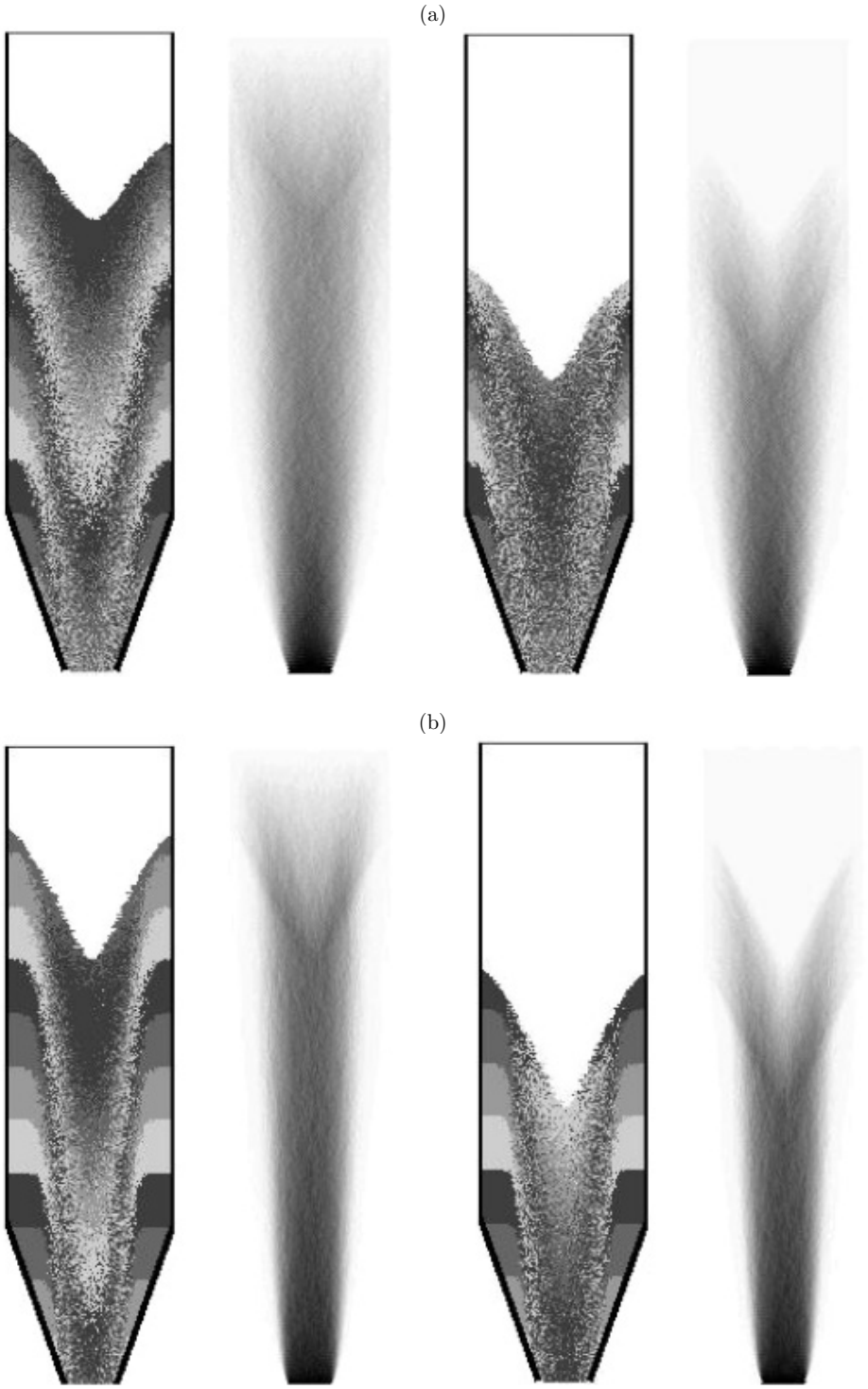

Figure 3. Flow patterns and distribution of flow rate during granular flow in a mass flow silo (migration rule **A** of Figure 1): (a) $p_1 = p_3 = 0.45$, $p_2 = 0.1$; (b) $p_1 = p_3 = 0.15$, $p_2 = 0.7$

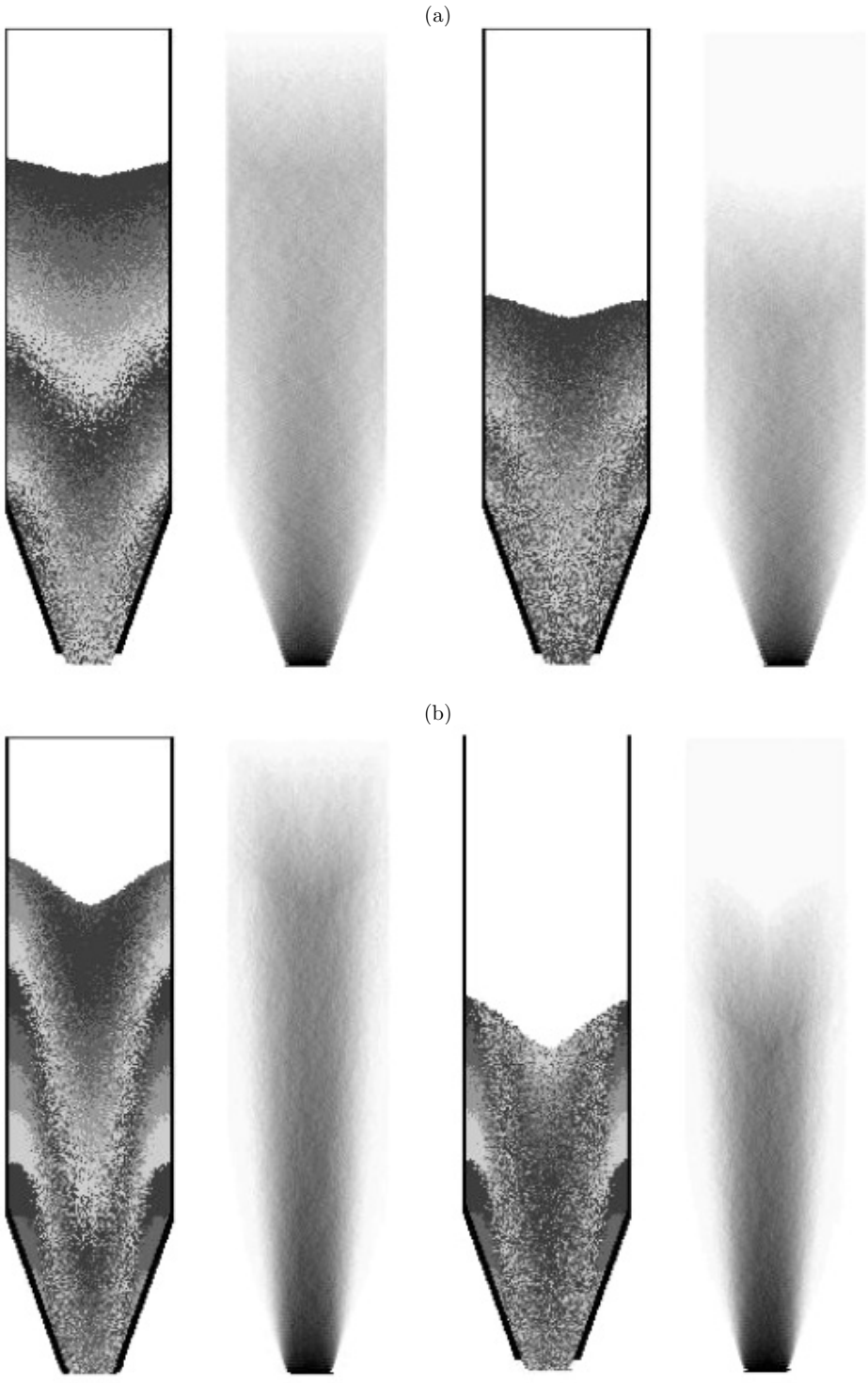

Figure 4. Flow patterns and distribution of flow rate during granular flow in a mass flow silo (migration rule **B** of Figure 1): (a) $p_1 = p_5 = 0.3$, $p_2 = p_4 = 0.15$, $p_3 = 0.1$; (b) $p_1 = p_5 = 0.05$, $p_2 = p_4 = 0.2$, $p_3 = 0.5$

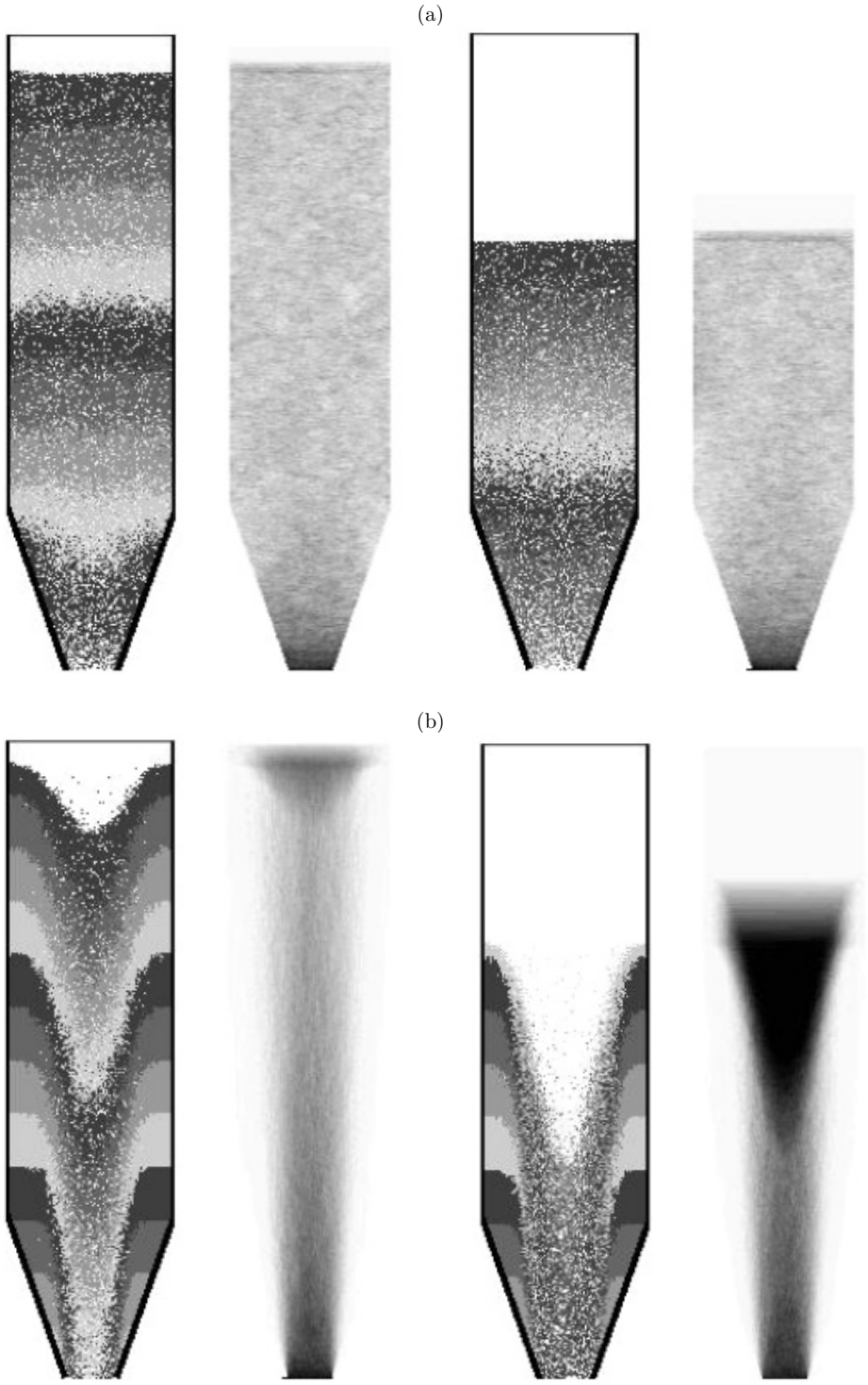

Figure 5. Flow patterns and distribution of flow rate during granular flow in a mass flow silo (migration rule **C** of Figure 1): (a) $p_1 = p_3 = 0.45$, $p_2 = 0.1$; (b) $p_1 = p_3 = 0.15$, $p_2 = 0.7$

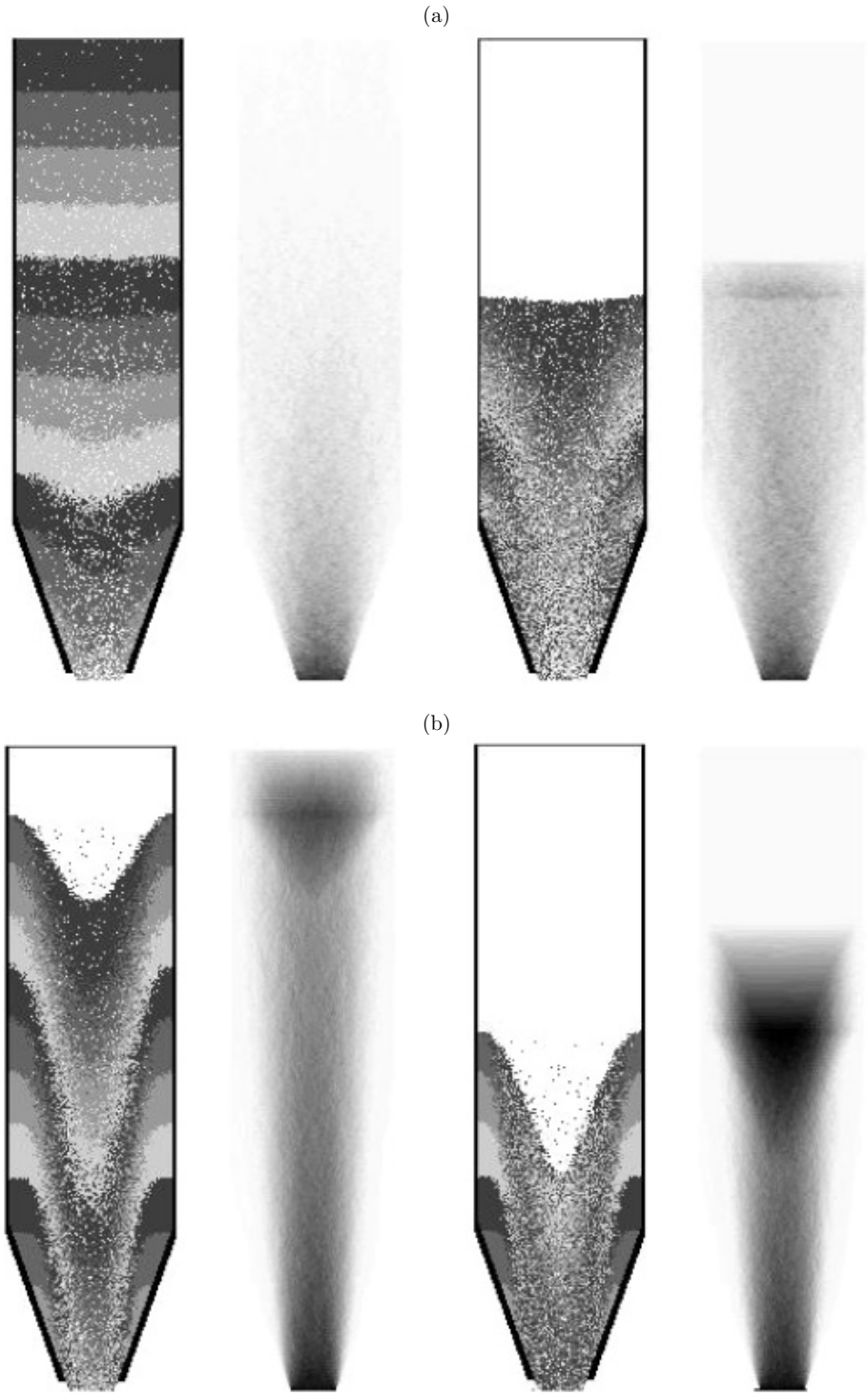

Figure 6. Flow patterns and distribution of flow rate during granular flow in a mass flow silo (migration rule **D** of Figure 1): (a) $p_1 = p_5 = 0.3$, $p_2 = p_4 = 0.15$, $p_3 = 0.1$; (b) $p_1 = p_5 = 0.05$, $p_2 = p_4 = 0.2$, $p_3 = 0.5$

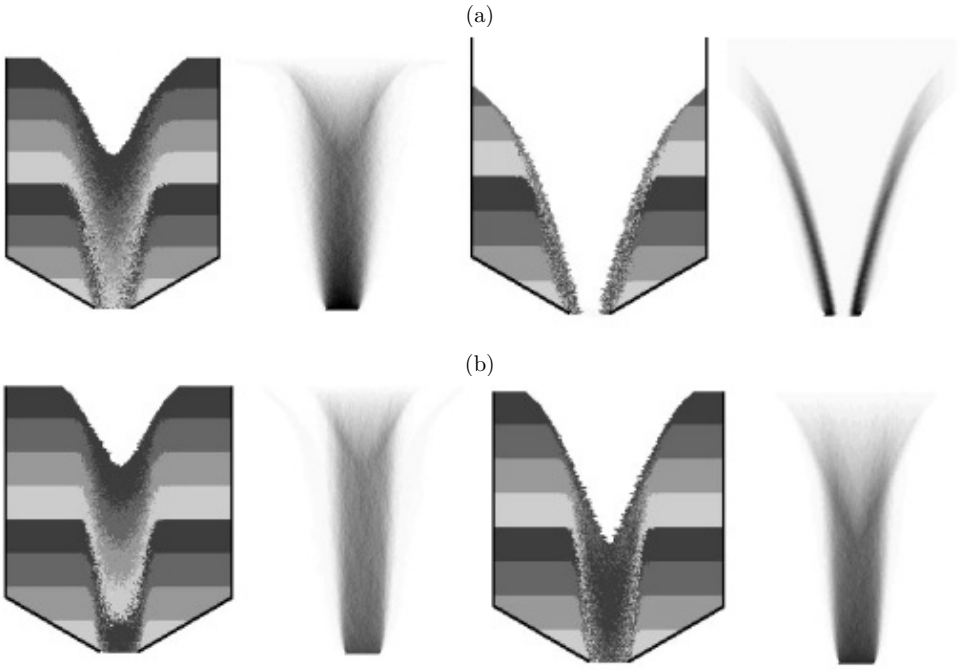

Figure 7. Flow patterns and distribution of flow rate during granular flow in a funnel flow silo (migration rule **A** of Figure 1): (a) $p_1 = p_3 = 0.45$, $p_2 = 0.1$, (b) $p_1 = p_3 = 0.15$, $p_2 = 0.7$

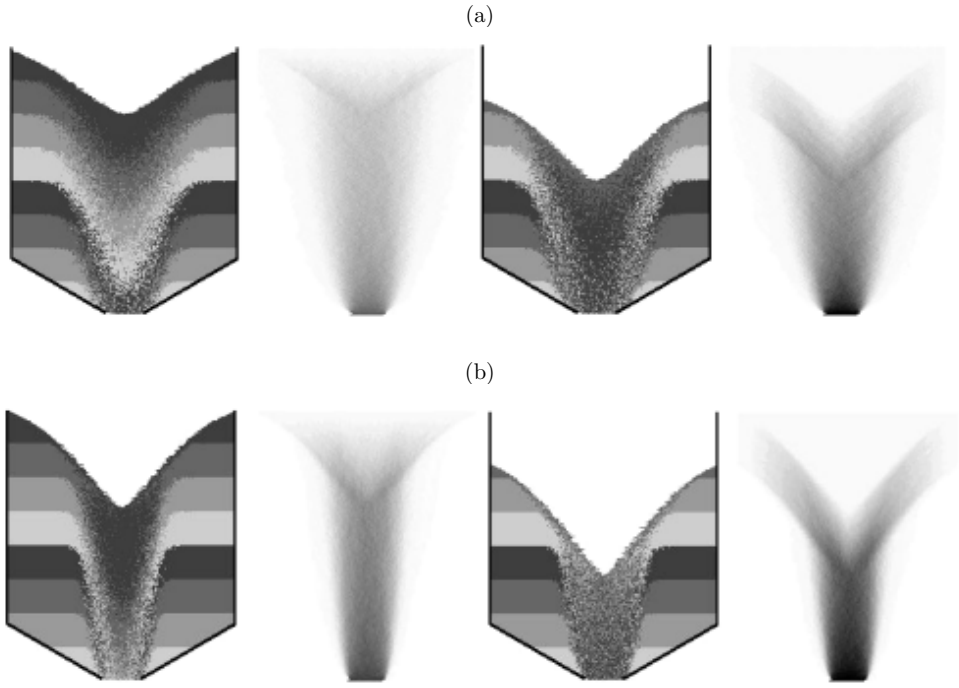

Figure 8. Flow patterns and distribution of flow rate during granular flow in a funnel flow silo (migration rule **B** of Figure 1): (a) $p_1 = p_5 = 0.3$, $p_2 = p_4 = 0.15$, $p_3 = 0.1$; (b) $p_1 = p_5 = 0.05$, $p_2 = p_4 = 0.2$, $p_3 = 0.5$

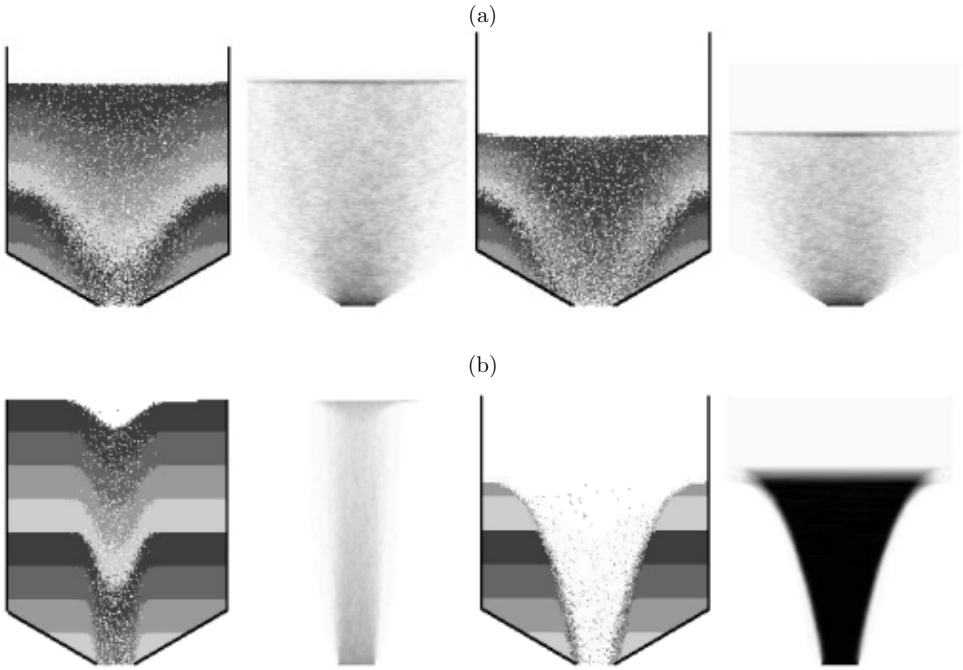

Figure 9. Flow patterns and distribution of flow rate during granular flow in a funnel flow silo (migration rule **C** of Figure 1): (a) $p_1 = p_3 = 0.45$, $p_2 = 0.1$; (b) $p_1 = p_3 = 0.15$, $p_2 = 0.7$

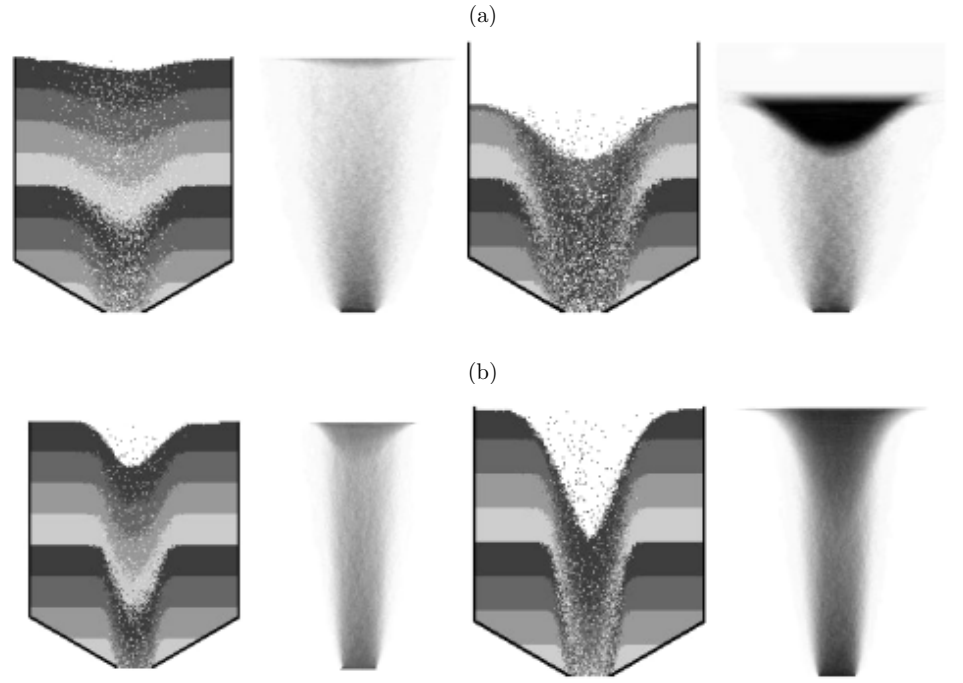

Figure 10. Flow patterns and distribution of flow rate during granular flow in a funnel flow silo (migration rule **D** of Figure 1): (a) $p_1 = p_5 = 0.3$, $p_2 = p_4 = 0.15$, $p_3 = 0.1$; (b) $p_1 = p_5 = 0.05$, $p_2 = p_4 = 0.2$, $p_3 = 0.5$

probability values near each void was assumed to be symmetric. The maximum values of p_i were assumed in the middle or at sides of cells. The following random probabilistic values were used ($\sum p_i = 1$): $p_1 = 0.45$, $p_2 = 0.1$, $p_3 = 0.45$ and $p_1 = 0.15$, $p_2 = 0.7$, $p_3 = 0.15$ (rule **A** and **C** of Figure 1), $p_1 = 0.3$, $p_2 = 0.15$, $p_3 = 0.1$, $p_4 = 0.15$, $p_5 = 0.3$ and $p_1 = 0.05$, $p_2 = 0.2$, $p_3 = 0.5$, $p_4 = 0.2$, $p_5 = 0.05$ (rule **B** and **D** of Figure 1). To visualize the simulation process, horizontal layers of various shades were introduced.

The results show that the effect of the migration rule on flow patterns is pronounced (Figures 3–10). The angle of repose of the granular material is the smallest for the migration rule **C** when the greatest probability values are at the sides of the row of cells above the void (Figures 5a and 9a), and the largest for the migration rule **D** when the greatest probability values are in the middle (Figures 6b and 10b). In general, the angle of repose increases when the probability values increase towards the mid-point. A satisfactory agreement of flow patterns with experimental results (for both flow types) occurs in the simulations with migration rule **B** and transition probabilities decreasing towards the mid-point (Figures 4a and 8a). To obtain an improved agreement, the transition probabilities should be calibrated better.

The flow rate evolution during silo discharge is shown in Figure 11 for the migration rule **B**. The mean flow rate is expressed by the overall number of cells going out of the silo outlet per iteration. At the beginning of discharge, a constant flow rate is observed throughout the run during both types of flow, in accordance with physical experiments [26, 27]. In the final phase of funnel flow, a non-linear reduction of the flow rate is obtained due to a successive decrease of the material volume in the silo. In the case of mass flow, a drastic reduction of the flow rate takes place.

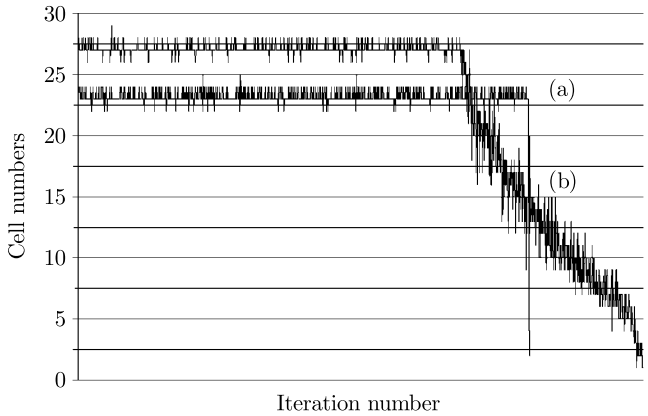

Figure 11. Calculated flow rate during granular flow in (a) mass and (b) funnel flow silos (migration rule **B** of Figure 1, $p_1 = p_5 = 0.3$, $p_2 = p_4 = 0.15$, $p_3 = 0.1$)

The calculation time for a silo flow with 50 000 cells using a 2.0 GHz PC was about 2 minutes.

3.2. Effect of the transport scheme

Figure 12 shows the results during 'disturbed' silo flow. Taking the flow of empty cells into account does not significantly influence the flow pattern. However, the material flows out more slowly.

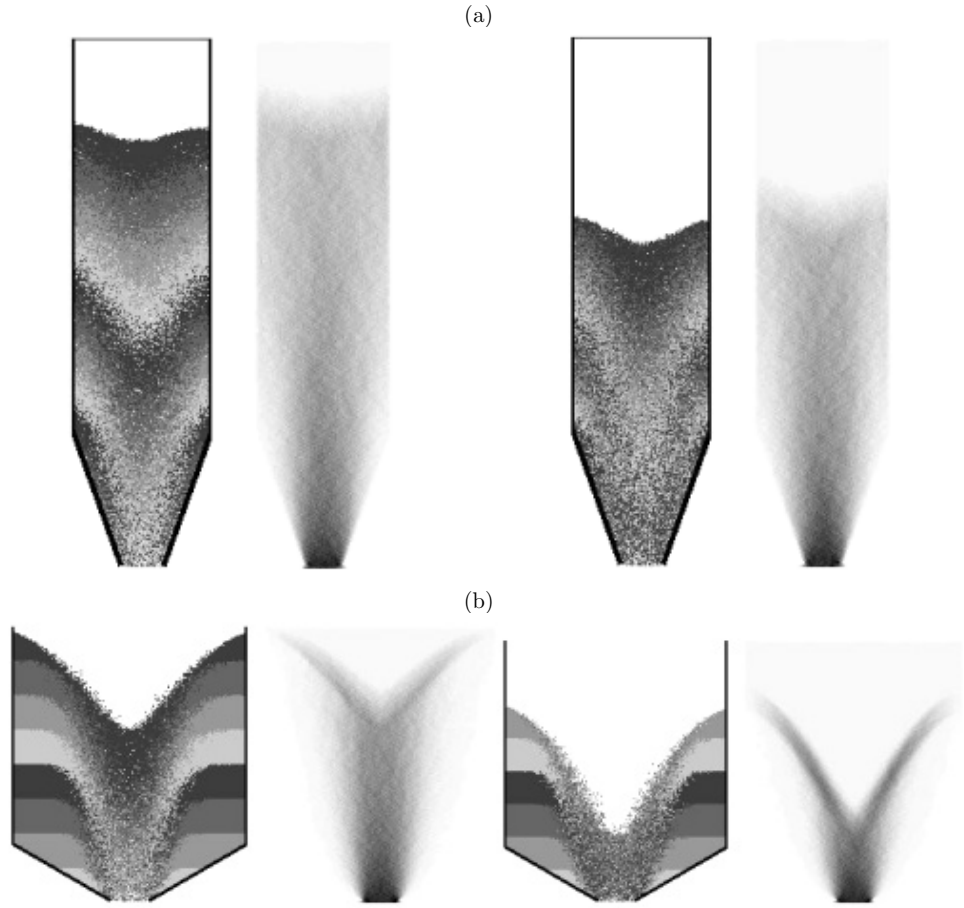

Figure 12. Flow patterns and distribution of flow rate during granular disturbed flow in (a) mass and (b) funnel flow silos (migration rule **B** of Figure 1, $p_1 = p_5 = 0.3$, $p_2 = p_4 = 0.15$, $p_3 = 0.1$)

3.3. Effect of outlet velocity

In Figure 13 results of silo flow with a constant outlet velocity are shown. The reduction in the outflow velocity diminishes the flow rate in the entire silo. The flow rate becomes more uniform, while the angle of repose of the granular material increases during mass flow and decreses during funnel flow.

3.4. Effect of wall roughness

The effect of increased wall roughness is presented in Figure 14. In this case, a different migration scheme was assumed in the wall region at the distance of 10 mm from the silo walls. The transition probability for flow was assumed to decrease there in accordance with a cosine function. The bulk material flows out more slowly. At the walls, there appears a narrow wall shear zone.

3.5. Effect of particle numbers

The effect of the number of cells during funnel flow silo is shown in Figure 15. The calculations were performed with 200 000 cells. The dimensions of cells were

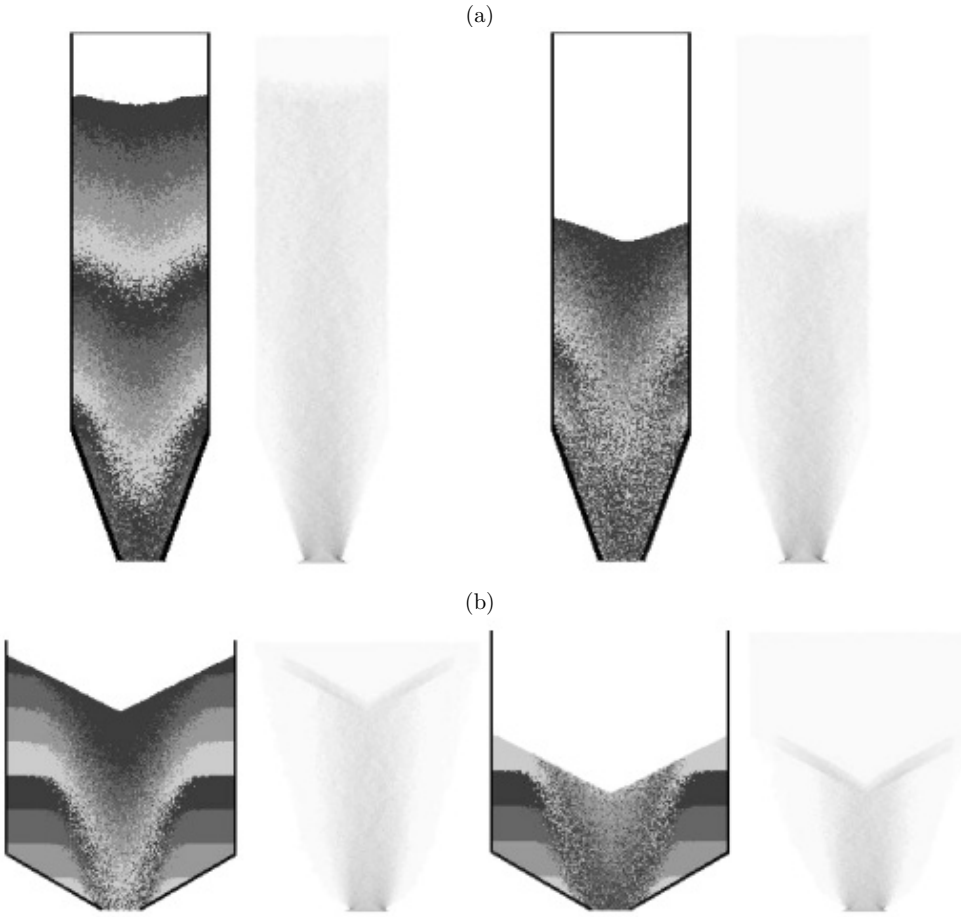

Figure 13. Flow patterns and distribution of flow rate during granular flow with a constant outlet velocity in (a) mass and (b) funnel flow silos (migration rule **B** of Figure 1, $p_1 = p_5 = 0.3$, $p_2 = p_4 = 0.15$, $p_3 = 0.1$)

$0.5 \times 0.5\,\mathrm{mm}^2$. An increase in the number of cells causes an increase of the granulate's angle of repose.

3.6. Effect of three-dimensional simulation

Three-dimensional calculations of flow patterns in the mass and funnel flow silo of Figure 2 were carried out with 3 500 000 cells by assuming the migration rule **B** of Figure 1 in both horizontal directions along the cross-section (Figure 16a), with $\sum p_i = 1$. In Figures 16b and 16c, the flow pattern in different horizontal sections is shown. The results are similar to those of two-dimensional calculations (due to the lack of wall friction). The calculation time using a 2.0 GHz PC was about 2.5 hours.

3.7. Effect of the lattice type

The effect of the lattice type is shown in Figures 17 and 18. The calculations were carried out with a hexagonal grid and the migration rule of Figure 17a for two different distributions of transition probability values (smaller at the sides and greater above the void or inversely). The agreement of results of the flow pattern is also

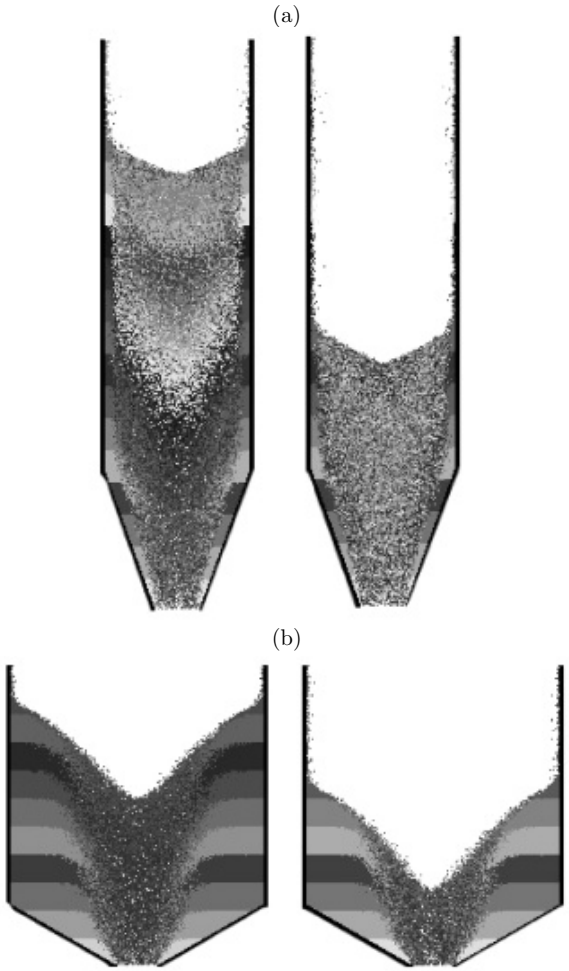

Figure 14. Flow patterns during granular flow with rough walls in (a) mass and (b) funnel flow silos (migration rule **B** of Figure 1, $p_1 = p_5 = 0.3$, $p_2 = p_4 = 0.15$, $p_3 = 0.1$)

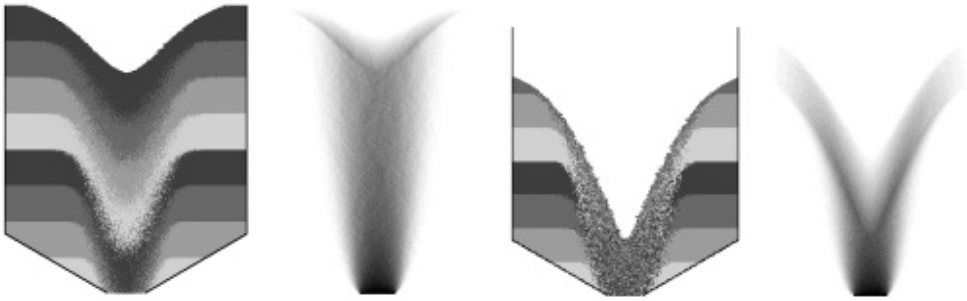

Figure 15. Flow patterns and distribution of flow rate during granular flow in a funnel flow silo (migration rule **B** of Figure 1, $p_1 = p_5 = 0.3$, $p_2 = p_4 = 0.15$, $p_3 = 0.1$, 200 000 cells)

satisfactory when compared with experiments (Figure 2). In the case of a hexagonal grid, the angle of repose decreases when transition probabilities are the greatest at the sides and increases when they are the smallest there (with respect to a quadratic grid).

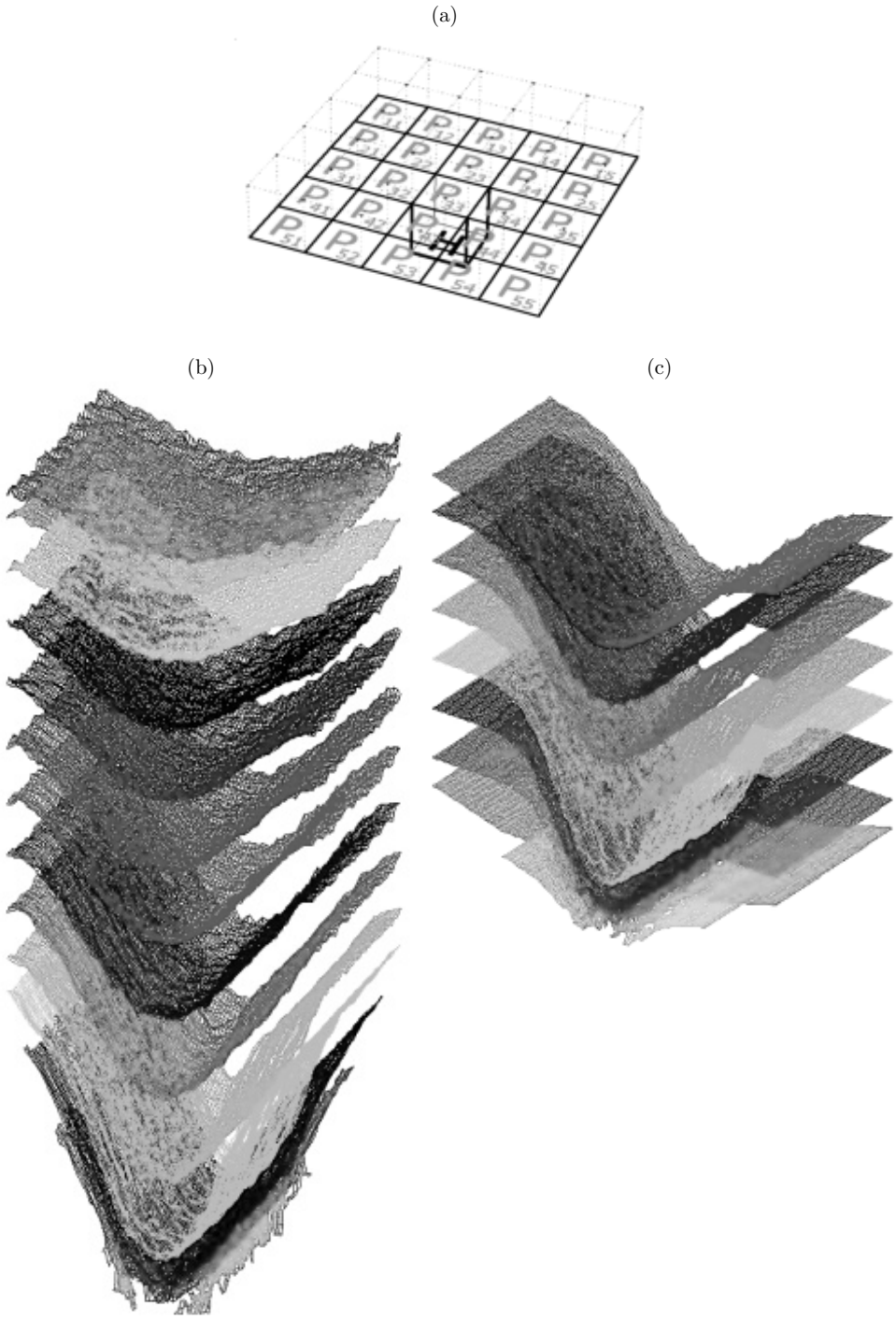

Figure 16. Migration rule (a) and flow patterns during three-dimensional granular flow in (b) mass and (c) funnel flow silos using quadratic cells ($p_{11} = p_{15} = p_{55} = p_{51} = 0.060$, $p_{12} = p_{21} = p_{14} = p_{25} = p_{41} = p_{45} = p_{54} = p_{52} = 0.053$, $p_{13} = p_{31} = p_{53} = p_{35} = 0.045$, $p_{22} = p_{42} = p_{44} = p_{24} = 0.023$, $p_{23} = p_{32} = p_{43} = p_{34} = 0.015$, $p_{33} = 0.003$)

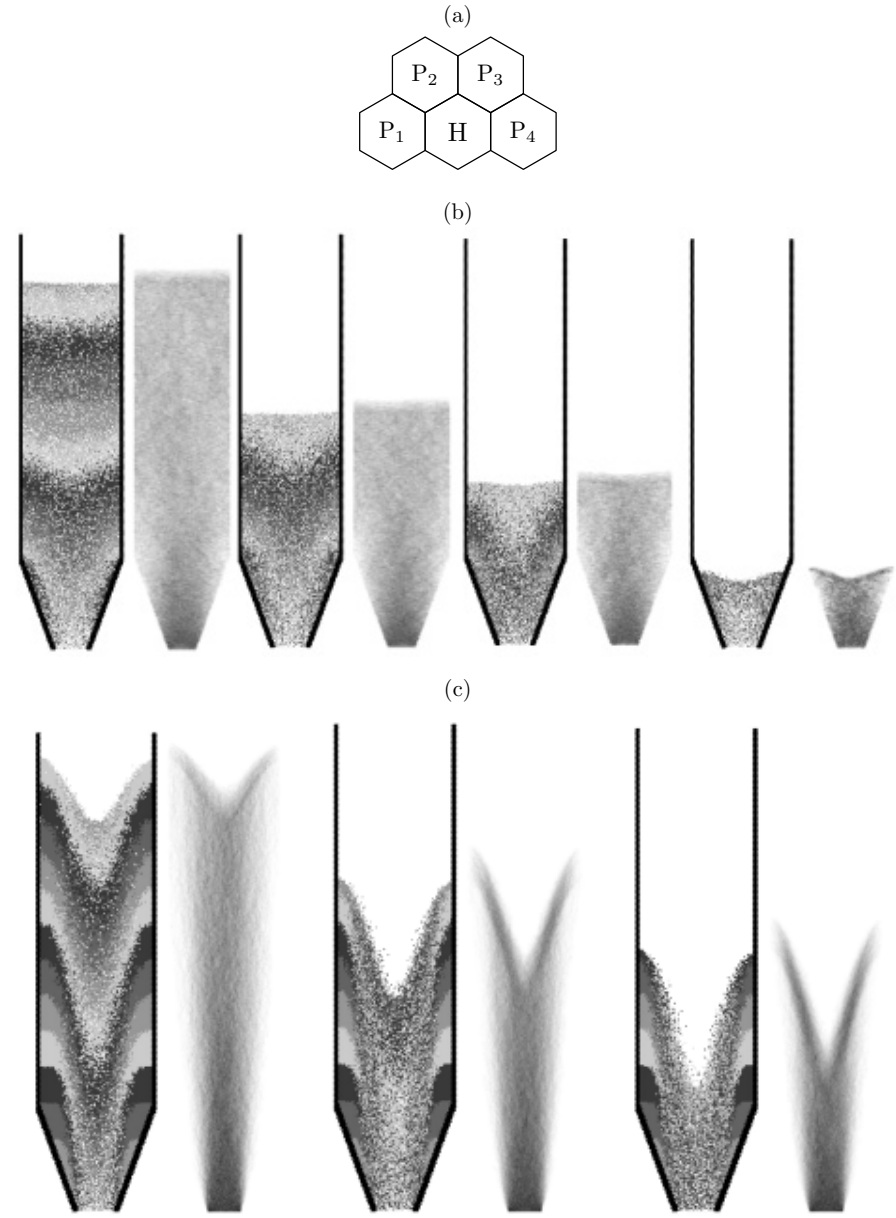

Figure 17. Migration rule (a), flow patterns and distribution of flow rate during granular flow in a mass flow silo (hexagonal grid): (b) $p_1 = p_4 = 0.4$, $p_2 = p_3 = 0.1$; (c) $p_1 = p_4 = 0.1$, $p_2 = p_3 = 0.4$

3.8. Effect of silo inserts

Silo inserts are used to improve the flow properties of bulk solids and to decrease silo wall pressures [24–26]. A wedge-shaped insert and an internal hopper change funnel flow into mass flow [28–30], while a perforated emptying tube [31, 32] or two inclined emptying tubes [33] change mass flow into funnel flow. When a wedge-shaped insert is located near the transition between the bin and the hopper, a significant reduction in pressures on the wall hopper is obtained [30]. An insert in the form of an

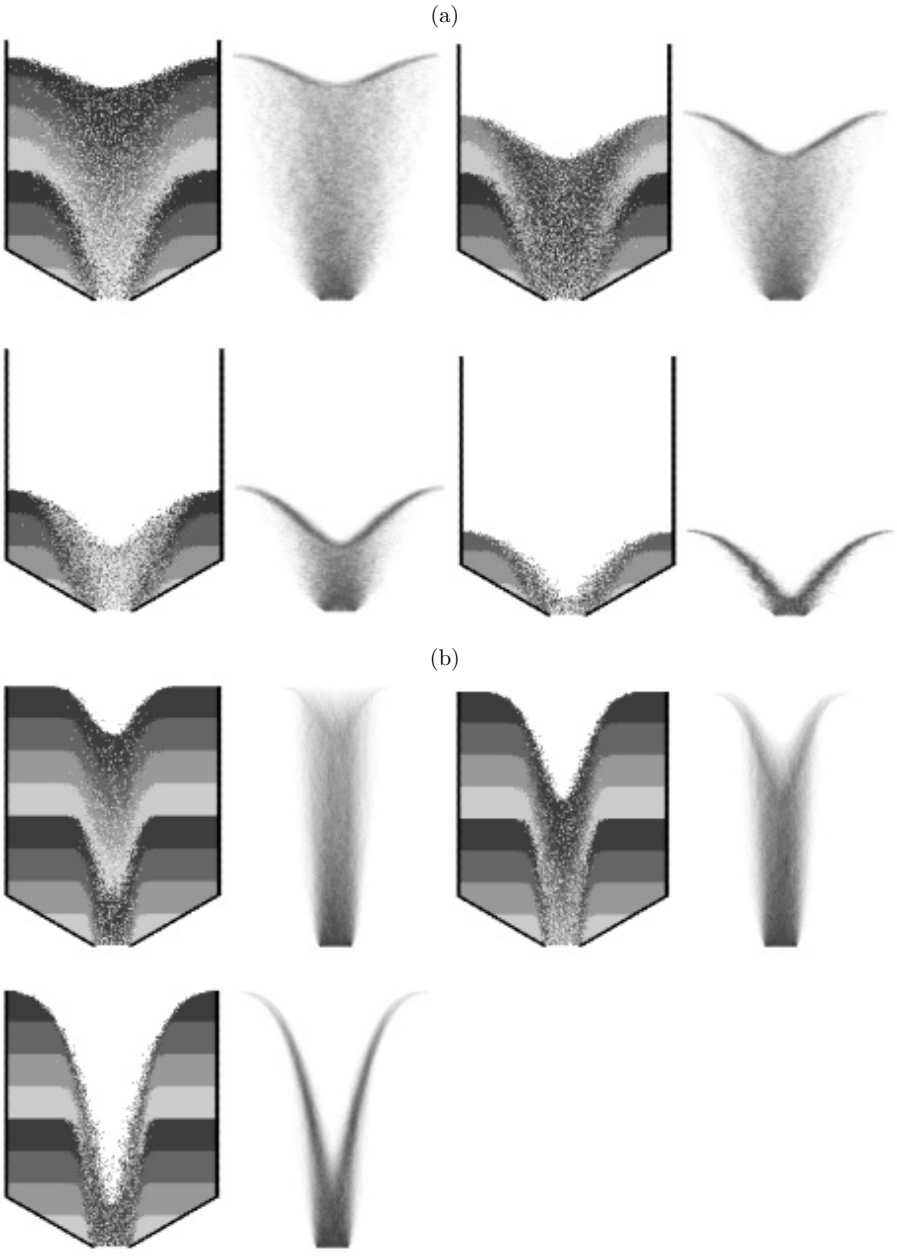

Figure 18. Flow patterns and distribution of flow rate during granular flow in a funnel flow silo (hexagonal grid): (a) $p_1 = p_4 = 0.4$, $p_2 = p_3 = 0.1$; (b) $p_1 = p_4 = 0.1$, $p_2 = p_3 = 0.4$

internal hopper inside the main hopper (the cone-in-cone concept) is applied to obtain mass flow at considerably large hopper inclinations at which funnel flow occurs [29, 30]. The outlet of the internal hopper is usually equal to the outlet of the main hopper. The flow pattern is affected mainly by the wall inclination of the internal hopper and the horizontal distance between the main and the internal hopper [30]. The perforated emptying tube (also called a depression column or an anti-dynamic tube) is hanged

in the middle of the silo or along the wall [25, 32]. It is usually made of steel and is connected to a silo's roof structure. It works only for non-cohesive materials. At the same time, two inclined discharging tubes are located symmetrically on the bin bottom [33]. Thanks to inserts of both of these types, a significant reduction of wall loads, flow rate and amplitude of dynamic pulsations is obtained due to the occurrence of funnel flow. In the case of too high pressures in silos, the method is cheaper than strengthening the silo structure with high-strength steel cables.

The calculations were carried out with a symmetric wedge-shaped insert located at two different heights of a funnel flow silo. During the analysis, 200 000 quadratic cells with the migration rule **B** of Figure 1 were used. The distribution of probability values was assumed to be symmetric with the largest values at both ends, diminishing towards the center of the layer above the void ($p_1 = p_5 = 0.3$, $p_2 = p_4 = 0.15$, $p_3 = 0.1$). Figure 19 demonstrates the flow patterns and distribution of flow rate during granular flow in a silo with a wedge-shaped insert. The presence of the insert, its size and position influence significantly the flow pattern and rate. Mass flow is obtained for the insert's position of Figure 19c.

The results for an internal hopper located at the transition between the bin and the main hopper are presented in Figure 20. During this analysis, 200 000 quadratic

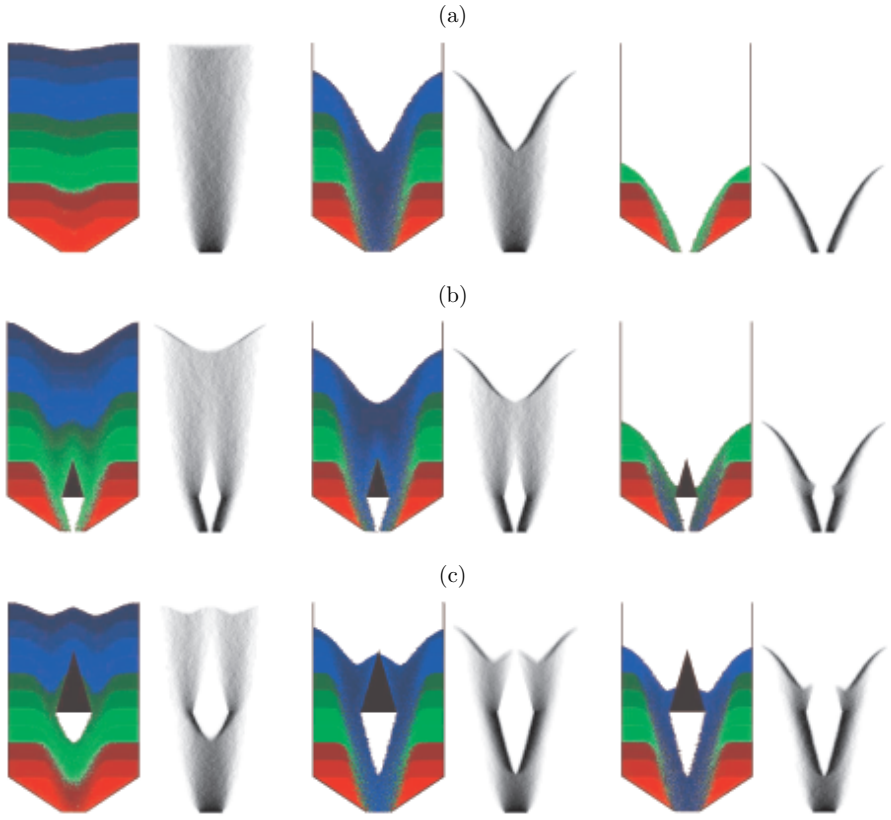

Figure 19. Flow patterns and distribution of flow rate during granular flow in a silo without and with inserts (quadratic cells, migration rule **B** of Figure 1): (a) silo without insert, (b) and (c) silo with insert ($p_1 = p_5 = 0.30$, $p_2 = p_4 = 0.15$, $p_3 = 0.1$)

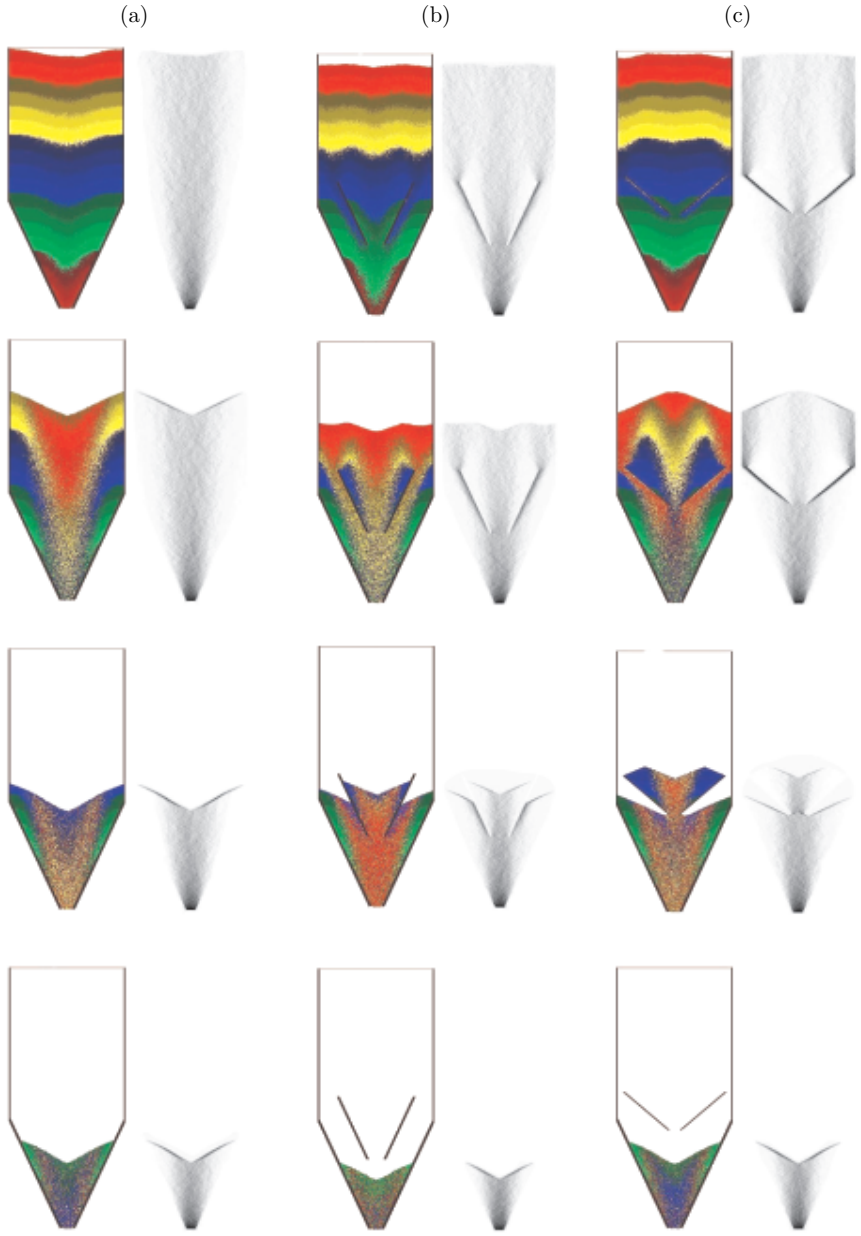

Figure 20. Flow patterns and distribution of flow rate during granular flow in a silo without an internal hopper (a) and with an internal hopper (b), (c) (quadratic cells, migration rule **B** of Figure 1, $p_1 = p_5 = 0.30$, $p_2 = p_4 = 0.15$, $p_3 = 0.1$)

cells were used (migration rule **B** of Figure 1). Two different wall inclinations of the internal hopper were assumed (Figures 20b and 20c). The flow in a silo without the internal hopper is of the funnel type (Figure 20a). The application of an internal hopper induces mass flow (Figures 20b and 20c), in accordance with experiments [30]. However, if the wall inclination of the internal hopper to the bottom is too small, the material flows too slowly in the center (Figure 20c).

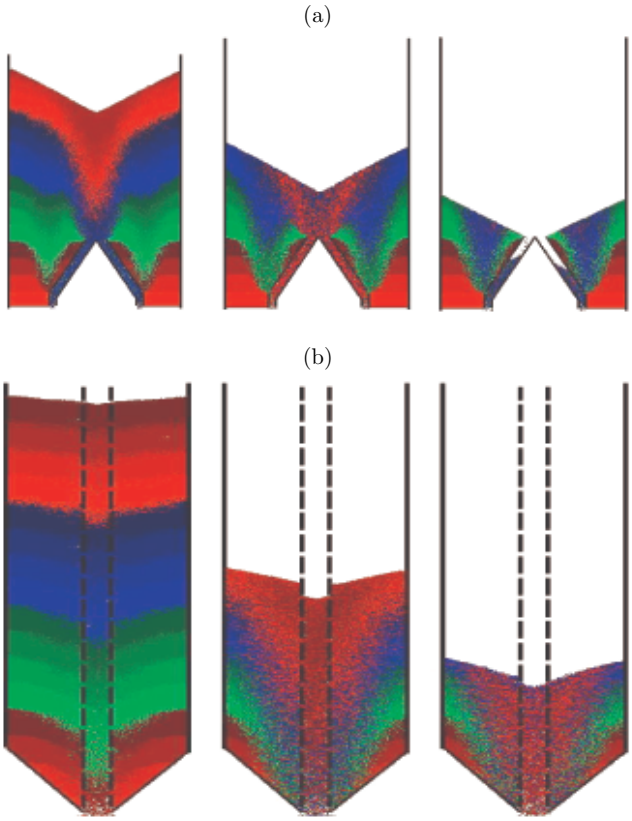

Figure 21. Flow patterns and distribution of flow rate during granular flow in a silo with two inclined tubes (a) and a silo with a perforate tube (b) (quadratic cells, migration rule **B** of Figure 1, $p_1 = p_5 = 0.3$, $p_2 = p_4 = 0.15$, $p_3 = 0.1$)

Figure 21 presents the calculated flow patterns in silos including two inclined tubes above the outlet and a perforated tube in the middle of the silo (200 000 quadratic cells, migration rule **B** of Figure 1). As the simulation results indicate, these two inserts promote funnel flow.

4. Conclusions

Cellular automata are purely kinematic models wherein flow dynamics is not taken into account. Although they are a gross oversimplification of real granular materials, they are capable of describing consistently the flow patterns of granulates in silos with and without inserts on the basis of a back analysis of experiments.

The main parameters governing the motion of granular particles in silos in the simplified cellular automaton discussed in this paper have been migration rules, transition probabilities, grid type and number of cells.

The migration rules assuming a decrease of transition probability values towards the mid-point of cells above the void have been able to capture the angle of repose of the bulk solid.

A simplified cellular automaton can be used to estimate the flow patterns of non-cohesive bulk materials in silos including inserts in the phase of the silo design.

References

[1] Chopard B, Droz B and Droz M 1998 *Cellular Automata Modeling of Physical Systems*, Cambridge University Press
[2] Ulm S 1952 *Proc. Int. Conf. Math.* **2** 264
[3] Litwiniszyn J 1956 *Archives of Appl. Mech.* **8** (4) 393
[4] Frisch U, Hasslacher B and Pomeau Y 1986 *Phys. Rev. Lett.* **56** 1505
[5] Caram H and Hong D C 1991 *Phys. Rev. Lett.* **67** 828
[6] Peng G and Herrmann H J 1994 *Phys. Rev.* **49** (3) 1796
[7] Fiske T J, Railkar S B and Kalyon D M 1994 *Powder Technology* **81** 57
[8] Sakaguchi H, Murakami A, Hasegawa T and Shirai A 1996 *Soils and Foundations* **36** (1) 105
[9] Hemmingson J, Herrmann H J and Roux S 1997 *J. Physique* **1** (7) 291
[10] Katsura N, Shimosaka A, Shirakawa Y and Hidaka Y 2001 *Powders and Grains* (Kishino, Ed.), Swets and Zeitlinger, Lisse, pp. 525–528
[11] Goles E, Gonzales G, Herrmann H and Martinez S 1998 *Granular Matter* **1** 137
[12] Murakami A, Sakaguchi H, Takasuka T and Fuji H 2001 *Powders and Grains* (Kishino, Ed.), Swets and Zeitlinger, Lisse, pp. 33–36
[13] Baxter G W, Behringer R P, Fagert T and Johnson G A 1990 *Pattern Formation and Time-dependence in Flowing Sand. Two Phase Flows and Waves* (Joseph D D and Schaeffer D G, Eds.), Springer Verlag, New York, pp. 1–29
[14] Baxter G W and Behringer R P 1991 *Physica* **D 51** 465
[15] Savage S B 1992 *Proc. Int. Conf. on Silos: Silos – Forschung and Praxis*, University of Karlsruhe, Germany, pp. 111–121
[16] Savage S B 1993 *Disorder and Granular Media* (Bideau D and Hansen A, Eds.), North-Holland, pp. 255–185
[17] Osinov V A 1994 *Continuum Mechanics and Thermodynamics* **6** 51
[18] Deserable D and Martinez J 1993 *Powder and Grains* (Thornton, Ed.), Balkema, pp. 345–350
[19] Martinez J, Masson S and Deserable D 1995 *Proc. Int. Conf. on Silos*, Partec 95, Nürnberg, pp. 367–379
[20] Deserable D, Masson S and Martinez J 2001 *Powders and Grains* (Kishino, Ed.), Swets and Zeitlinger, Lisse, pp. 421–424
[21] Kozicki J and Tejchman J 2002 *TASK Quart.* **6** (3) 429
[22] Tejchman J and Klisinski M 2001 *Granular Matter* **3** (4) 215
[23] *Silo Standard: Lastannahmen für Bauten*, DIN 1055, Teil 6, 1987
[24] Pieper K and Wagner K 1968 *Aufbereitungstechnik* **10** 542
[25] Safarian S S and Harris E C 1985 *Design Construction of Silos and Bunkers*, Von Nostrand Reinhold Company
[26] Hampe E 1987 *Silos*, VEB Verlag für Bauwesen, Berlin
[27] Schwedes J 1999 *Lagern und Fließen von Schüttgütern. Hochschulkurs*, Script, University of Braunschweig
[28] Strusch J, Schwedes J and Hardow B 1995 *Proc. Int. Conf. on Silos*, Partec 95, Nürnberg, pp. 163–182
[29] Johanson J R 1982 *Bulk Solid Handling* **2** (3) 11
[30] Eiksa O E, Mosby J and Enstad E E 1995 *Proc. Int. Conf. on Silos*, Partec 95, Nürnberg, pp. 417–426
[31] Reimbert M and Reimbert A 1976 *Silos – Theory and Practice*, Trans. Tech. Publishing, Clausthal, Germany
[32] Kamiński M and Zubrzycki M 1985 *Reduzieren des dynamischen Horizontaldruckes in Getreidesilos*, Bauingenieur, pp. 313–318
[33] Kamiński M and Antonowicz R 2003 *TASK Quart.* **7** (4) 561